THE GERONTOLOGICAL SOCIETY OF AMERICA®

Journals of Gerontology: Biological Sciences
cite as: *J Gerontol A Biol Sci Med Sci*, 2019, Vol. XX, No. XX, 1–8
doi:10.1093/gerona/glz153
Advance Access publication June 14, 2019

OXFORD

Original Article

The Effects of Metformin on Age-Related Changes in the Liver Sinusoidal Endothelial Cell

Nicholas J. Hunt, PhD,[1,2,3,4] Glen P. Lockwood, BSc,[1,2,4] Sun Woo (Sophie) Kang, PhD,[1,2,4] Tamara Pulpitel, PhD,[4] Ximonie Clark, PhD,[4] Hong Mao, MSc,[5] Peter A. G. McCourt, PhD,[4,5] Gregory J. Cooney, PhD,[4] Jibran A. Wali, PhD,[2,4,6] Frank H. Le Couteur,[1] David G. Le Couteur, MD, PhD,[1,2,3,4,] and Victoria C. Cogger, PhD[1,2,3,4,*]

[1]ANZAC Research Institute, Biogerontology Laboratory and [2]Aging and Alzheimer's Institute and Centre for Education and Research on Ageing, Concord Repatriation General Hospital, New South Wales, Australia. [3]Concord Clinical School, Sydney Medical School and [4]Charles Perkins Centre, Nutritional Ecology and Physiology Laboratory, The University of Sydney, New South Wales, Australia. [5]Department of Medical Biology, University of Tromsø - The Arctic University of Norway. [6]Faculty of Science, School of Life and Environmental Sciences, The University of Sydney, New South Wales, Australia.

*Address correspondence to: Victoria C. Cogger, PhD, Centre for Education and Research on Ageing, Concord Repatriation General Hospital, Sydney, Australia. E-mail: victoria.cogger@sydney.edu.au

Received: March 21, 2019; Editorial Decision Date: June 2, 2019

Decision Editor: Rozalyn Anderson, PhD

Abstract

Age-related changes in the liver sinusoidal endothelium, particularly the reduction in fenestrations, contribute to insulin resistance in old age. Metformin impacts on the aging process and improves insulin resistance. Therefore, the effects of metformin on the liver sinusoidal endothelium were studied. Metformin increased fenestrations in liver sinusoidal endothelial cells isolated from both young and old mice. Mice administered metformin in the diet for 12 months had increased fenestrations and this was associated with lower insulin levels. The effect of metformin on fenestrations was blocked by inhibitors of AMP-activated protein kinase (AMPK), endothelial nitric oxide synthase, and myosin light chain kinase phosphorylation. Metformin led to increased transgelin expression and structural changes in the actin cytoskeleton but had no effect on lactate production. Metformin also generated fenestration-like structures in SK-Hep1 cells, a liver endothelial cell line, and this was associated with increased ATP, cGMP, and mitochondrial activity. In conclusion, metformin ameliorates age-related changes in the liver sinusoidal endothelial cell via AMPK and endothelial nitric oxide pathways, which might promote insulin sensitivity in the liver, particularly in old age.

Keywords: NOS, LSEC, dSTORM, Aging, Insulin

Metformin is prescribed for type 2 diabetes mellitus and delays aging via effects on nutrient sensing pathways (1–3). Its mode of action is unclear but involves activation of AMP-activated protein kinase (AMPK) secondary to inhibition of mitochondrial respiratory activity (4). The primary target organ of metformin is the liver (5,6) where metformin downregulates protein synthesis (7), lipogenesis (8,9), and gluconeogenesis (10), and upregulates insulin signaling (8,11).

Aging is associated with a number of changes in liver function and structure, including hepatic insulin resistance (1,12–15). We found that old age leads to changes in the liver sinusoidal endothelial cells (LSEC), which may contribute to hepatic insulin resistance. LSECs have a unique morphology including the presence of fenestrations which are transcellular pores that facilitate the transfer of substrates such as insulin between blood and hepatocytes. With old age, there is a reduction in fenestrations associated with thickening of the

endothelium, upregulation of endothelial markers, and perivascular deposition of collagen and basal lamina (15,16). These age-related changes, termed "pseudocapillarization," impair the uptake of insulin leading to hepatic insulin resistance and reduced clearance of insulin (14,15).

Here, we investigated the effects of metformin on fenestrations in old age, and mechanisms for the effects of metformin on LSECs. We also studied the molecular pathways promoted by metformin in and SK-Hep1 cells, an immortal human liver cell line that shares many of the features of LSECs.

Methods

Ethics

The study was approved by the Animal Welfare Committee of the Sydney Local Health District and was performed in accordance with the Australian Code of Practice for the care and use of animals for scientific research (AWC: 2016/009, 2018/010). All information provided accords with ARRIVE guidelines.

Reagents

Cell/tissue culture: collagenase (Type 1, cat no: 47D17410A, ProSciTech, Australia), RPMI-1640 (cat no: R0883, Sigma–Aldrich, Australia), Percoll (cat no: P4937, Sigma–Aldrich), 1,1-Dimethylbiguanide hydrochloride (metformin cat no: D150959, Sigma–Aldrich), Dulbecco's modified Eagle medium (cat no: M8042, Sigma–Aldrich), penicillin–streptomycin (cat no: P4333, Sigma–Aldrich), fetal calf serum (cat no: F2442, Sigma–Aldrich), Dorsomorphin dihydrochloride (Compound C, cat no: ab144821, Abcam, Australia), Myosin Light Chain Kinase Inhibitor Peptide 18 (cat no: 475981, Merck, Australia), Nω-Nitro-L-arginine methyl ester hydrochloride (cat no: N5751, Sigma–Aldrich). Assays were performed using In Vitro Toxicology Assay Kit, MTT based (cat no: TOX1-1KT, Sigma–Aldrich), cyclic guanosine monophosphate (cGMP) ELISA kit (cat no: 581021, Sapphire Bioscience, Australia), ATP bioluminescence assay kit (cat no: A22066, ThermoFisher, Australia), L-lactate assay kit (cat no: 700510, Sapphire Bioscience, Australia), and mouse insulin ELISA kit (cat no: 90080, Crystal Chem Inc, IL). Antibodies: p-AMPKα (Thr172, cat no: 2531, Cell signaling Technology, Australia), AMPKα (cat no: 2532, Australian Biosearch, Australia), anti-p-eNOS (Ser1177, cat no: 9571, Genesearch, Australia), anti-eNOS (type 3, cat no: 610296, BD Bioscience, Australia), transgelin (anti-SM22 alpha antibody; cat no: ab14106, Abcam), Alexa Fluor 488 phalloidin (cat no: A12379, Thermo Fisher, Australia), Alexa Fluor 488 Goat anti-Rabbit (cat no: R-37116; Thermo Fisher), MitotrackerGreen (cat no: M7514, Thermo Fisher), and TMRE (cat no: T669, Thermo Fisher). Western blot reagents: loading buffer (cat no: B0007, Thermo Fisher), running buffer (cat no: B0001, Thermo Fisher), transfer buffer (cat no: BT00061, Thermo Fisher), Ponceau staining (cat no: P7170, Sigma–Aldrich), PBS tablets (cat no: P4417, Sigma–Aldrich), and Tween-20 (cat no: P1379, Sigma–Aldrich).

In Vitro Cell Culture Studies

Three to four (n = 3) and 18 (n = 3)-month-old male C57/Bl6 mice were obtained from the Animal Resource Centre in Perth, Western Australia; and housed at the ANZAC Research Institute (Concord Repatriation General Hospital, NSW, Australia). Mice were group housed, maintained on a 12-hour light/dark cycle, 20–25°C, 50%–60% relative humidity and provided with bedding, ventilated caging systems, and enrichment as per the ARRIVE guidelines. The Mice were anesthetized with ketamine and xylazine (100 mg/kg; 10 mg/kg). LSECs were isolated and cultured as described (17–19). In brief, livers were perfused with collagenase and parenchymal cells were removed by a two-step Percoll gradient. Küpffer cells were removed by selective adherence to plastic. LSECs were then cultured (37°C, 5% CO_2) in serum-free RPMI-1640 for 3.5 hours before use.

SK-Hep1 cells were obtained from the American Type Tissue Culture Collection (ATCC, Manassas, VA). Cells were cultured (37°C, 5% CO2) in Dulbecco's modified Eagle medium supplemented with 10% fetal calf serum and penicillin–streptomycin. Cells were plated in flasks coated with (0.2 mg/mL) fibronectin.

LSECs and SK-Hep1 cells were incubated with metformin concentrations at 5, 10, 25, 50, and 100 μM in RPMI media for 30 minutes. These concentrations were based on previous studies (3,20,21).

The effects of metformin on fenestrations were evaluated using scanning electron microscopy (SEM). SEM was performed as previous described using a JEOL 6380 Scanning Electron Microscope (JEOL Ltd, Japan) (17–19). Images at 10,000× magnification were captured and analyzed for: (i) fenestration porosity (defined as the percentage of the cell membrane covered with fenestrations relative to the total cell surface, excluding the nucleus area), (ii) fenestration diameter, and (iii) fenestration frequency (defined at the number of fenestrations per 1 μm^2 per total cell surface). Between 1,713 and 3,278 fenestrations were counted per treatment group, per mouse (8–16 images per mouse, minimum 3 mice per treatment) by a observer blinded to the age and treatment group. Fenestrations less than 30 nm and gaps more than 300 nm were excluded from analysis similarly to our previous publication (19).

The effects of metformin on transgelin and the actin cytoskeleton were evaluated using direct stochastic optical reconstruction microscopy (dSTORM). Paraformaldehyde-fixed cells were stained with either Alexa Flour phalloidin 488 (1:40, 20 minutes) or transgelin (1:100, 16 hours 4°C) followed by Alexa Fluor 488 Goat anti-Rabbit (1:1,000, 2 hours). dSTORM used a 488 nm excitation from diode-pumped lasers (Coherent Inc, California). Excitation was delivered via a 1.49NA 60× oil-immersion TIRF objective (Olympus Australia, Australia). Fluorescence was captured on an industrial CMOS camera (Imaging Development Systems GmbH, Germany). Data were collected for up to 40,000 images at 75 fps. Eight whole cell images were collected for each treatment dosage and processed using RapidSTORM open source software (22). Densitometry measurements were performed using eight dSTORM images with data analysis performed using Image J software (National Institute of Heath, Maryland) similarly to our previous publication (19).

Potential mechanisms for the effects of metformin in vitro were explored using several methods. Isolated LSECs were pretreated with Peptide 18 (100 μM, 45 minutes) (23), Compound C (10 μM, 20 minutes) (6) or N(ω)-nitro-L-arginine methyl ester (L-NAME) (3 mM, 30 minutes) (24) to inhibit phosphorylated myosin light chain kinase (MLCK), phosphorylated AMPK, and endothelial nitric oxide synthase (NOS), respectively. Mitochondrial membrane potential was measured using tetramethylrhodamine, ethyl ester (TMRE) (100 nM, 10 minutes), and MitotrackerGreen (250 nM, 15 minutes) and imaged with a Leica SP8 inverted scanning confocal microscope with Type F immersion oil (cat. no. 11513859) and images captured using LAS software (Leica Microsystems CMS, Wetzlar, Germany) (25,26). SK-Hep1 cell lines were used for cGMP, L-lactate, ATP, and MTT assays that were performed as described elsewhere (19,25). Western blots for p-AMPK, AMPK, p-eNOS, and NOS with actin and Ponceau controls performed as previously described (25,26).

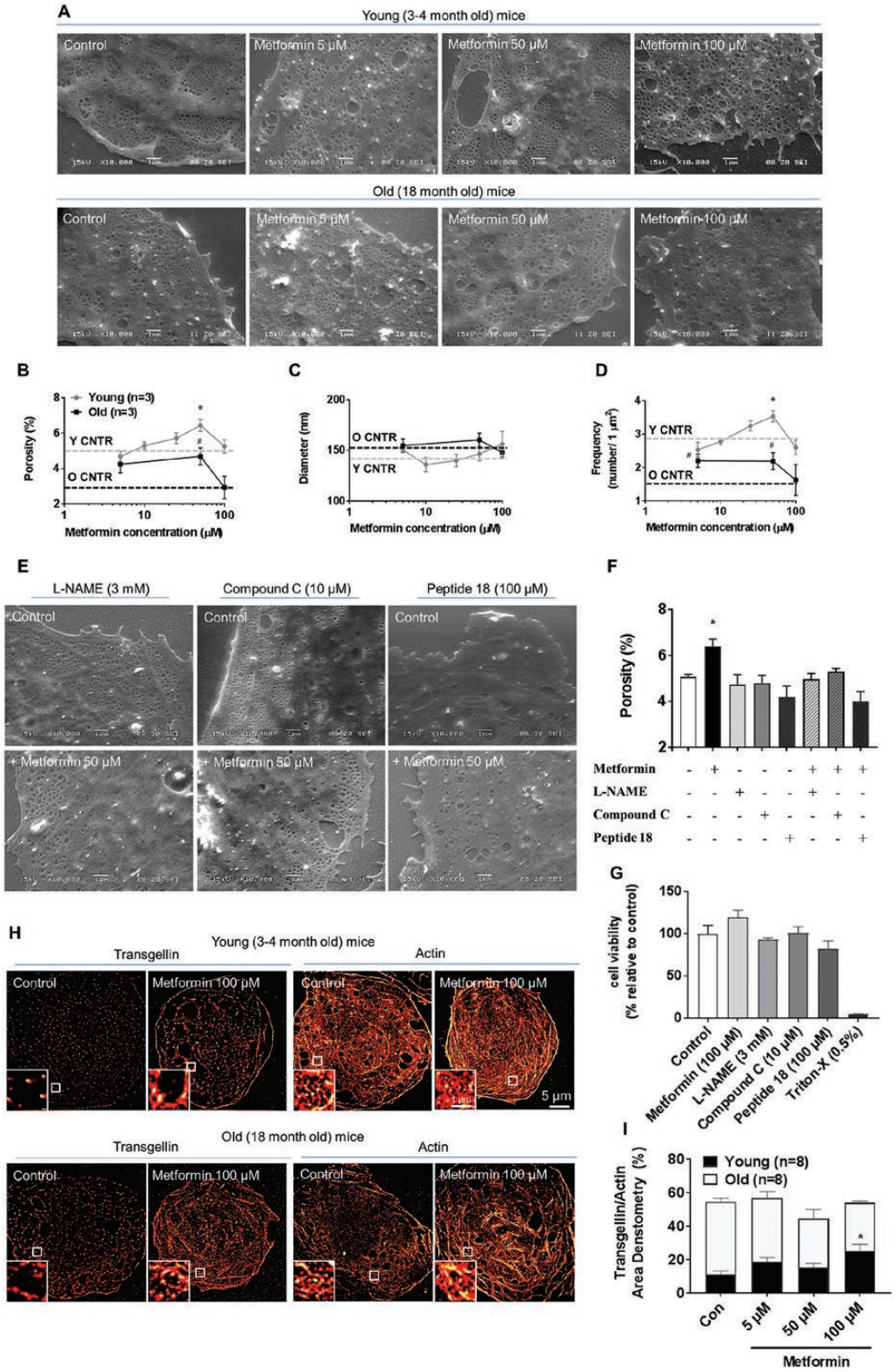

Figure 1. Effects of metformin on isolated young and old mice liver sinusoidal endothelial cells. (**a**) Representative scanning electron microscopy (SEM) images following metformin treatment in young and old mice. Scale bars show 1 μm. (**b–d**) Dose–response curves showing changes in fenestration porosity (**b**), diameter (**c**), and frequency (**e**) with increasing dosage of metformin. Solid gray line shows young mice data, black line shows is old mice data. Gray and blank dotted lines show the mean control (untreated) score. All data show the mean ± *SD* with the metformin concentration shown with a log 10 scale. Porosity is shown as the percentage area occupied by fenestrations relative to the total cell area excluding the nucleus, and frequency shows the number of fenestrations per 1 μm². *, # indicates a *p*-value of < .05 compared to young (*) or old (#) control data. All statistics were performed using Kruskal–Wallis with post hoc Dunn's test to compare between groups, *n* = 3 (biological replicates) for all groups. All data were collected using 1,988–3,278 (young) or 1,713–2,345 (old)

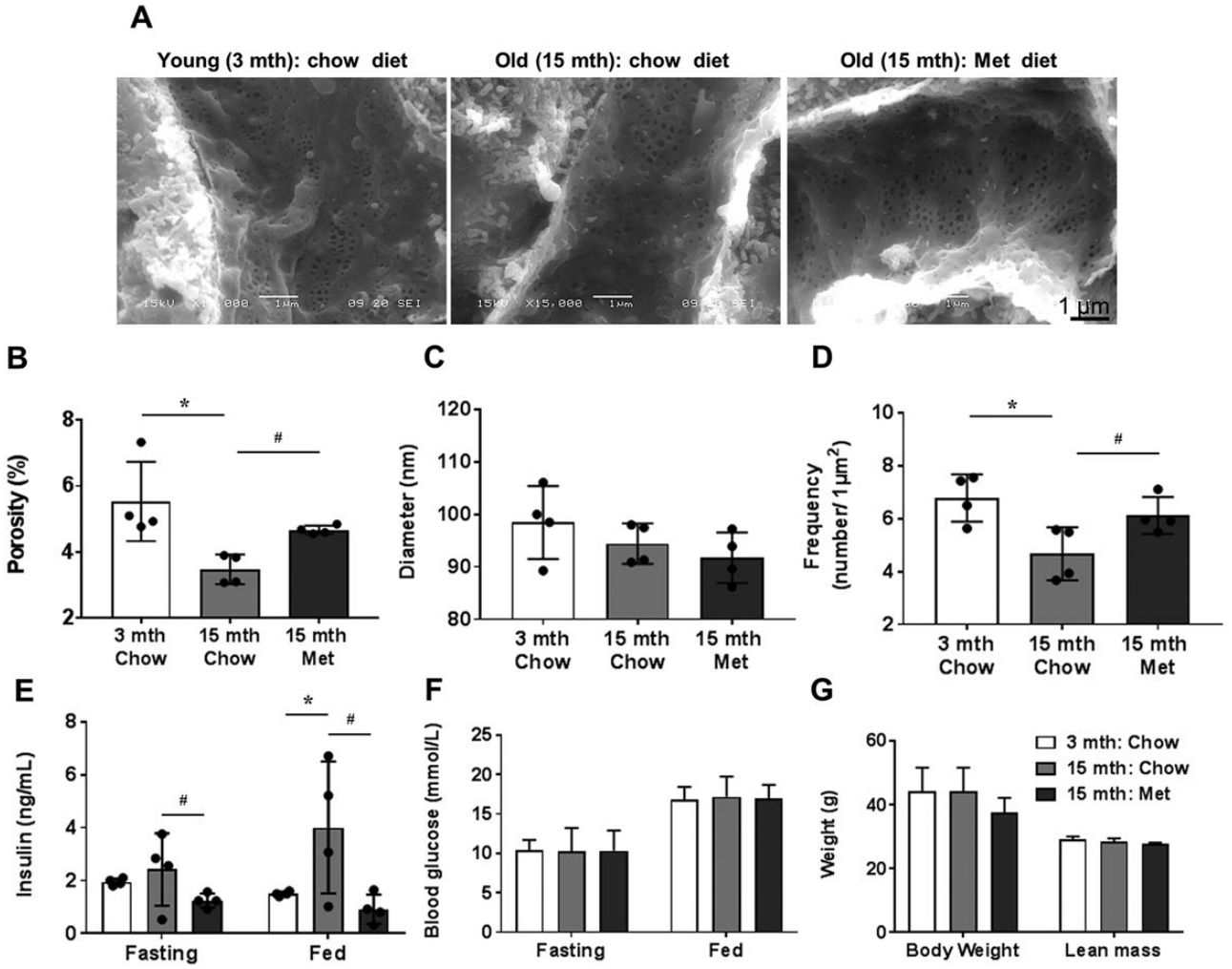

Figure 2. Effects of fenestrations and circulating insulin following 12 months 0.1% metformin diet. (**a**) Sample scanning electron microscopy images of in vivo liver sinusoidal endothelial cells from chow-fed 3-month (left) and 15-month (middle)-old mice. Panel of right shows a 15-month-old mouse fed 0.1% metformin for 12 months. Scale bar shows 1 μm. (**b–d**) Changes in fenestration porosity (**b**), diameter (**c**), and frequency (**d**) between chow fed young mice, old mice; and old mice fed metformin diet. All data show the mean ± *SD*. All data were collected using 749–1,571 fenestration raw data points (per mouse). Statistics were performed using Kruskal–Wallis with post hoc Dunn's test to compare between groups, $n = 4$ (biological replicates) for all groups. *, # indicates a p-value of < .05 compared to 3-month chow fed (*) or 15-month chow fed (#). Porosity is shown as the percentage area occupied by fenestrations relative to the total cell area, diameter is given in nm and frequency shows the number of fenestrations per 1 μm^2. (**e**) Changes in fasting and fed blood insulin between chow fed young mice (3 months; white bars) old mice (15 months, gray bars) and metformin fed old mice (15 months, black bars). Insulin measures were performed using 10 μL of whole blood from fasted mice (5 hours.) and again following an oral bolus of 25% glucose solution. All data show the mean ± *SD*. Statistics were performed using Kruskal–Wallis with post hoc Dunn's test to compare between groups, $n = 4$ for all groups. *, # indicates a p-value of < .05 compared to 3-month chow fed (*) or 15-month chow fed (#). (**f**) Changes in fasting and fed blood glucose between chow fed young mice (3 months; white bars) old mice (15 months, gray bars) and metformin-fed old mice (15 months, black bars). Blood glucose measures were performed on a hand-held glucose meter using 10 μL of blood. Mice were tested fasting and 15 minutes after feeding. All data show the mean ± *SD*. $n = 4$ for all groups. (**g**) Body weight and lean mass comparisons between young mice (3 months; white bars) old mice (15 months, gray bars) and metformin-fed old mice (15 months, black bars). All data show the mean ± *SD*. $n = 4$ for all groups.

raw measurements of fenestrations (per drug treatment, per mouse) and analyzed using ImageJ software. (**e**) Representative SEM images following inhibitor pretreatment alone and following 50 μM metformin drug treatment. Scale bars show 1 μm. (**f**) Changes in porosity following 50 μM metformin treatment with and without pretreatment with L-NAME, Compound C or Peptide 18. Data are presented as a bar graph (mean ± *SD*), * indicates a p-value of < .05 compared to young control data. All statistics were performed using Kruskal–Wallis with post hoc Dunn's test to compare between groups, $n = 3$ for all groups. All data were collected using 1,231–2,658 raw measurements of fenestrations (per drug treatment, per mouse) and analyzed using ImageJ software. (**g**) Cell viability as determined by MTT assays as per kit instructions following metformin, L-NAME, Compound C, Peptide 18 or Triton-X (negative control) treatments. Data shows mean ± *SD* with all experiments performed in triplicate. (**h**) dSTORM images show transgelin and actin cytoskeleton morphology changes promoted by metformin drug treatment in young and old mice. Images were produced following 40,000 image collections and processed using RapidSTORM software. Scale bar shown 5 μm, insert scale bar 1 μm. (**i**) Changes in transgelin densitometry relative to actin densitometry induced by metformin treatments in young and old mice. Data are presented as a bar graph (mean ± *SD*) with the percentage density of pixels per 1 μm^2. Eight images were captured using a dSTORM microscope; data analysis was performed using Image J software. Images were converted to binary data with measurements taken across the whole cell. * indicates a p-value of < .05 compared to young control data; eight images per treatment group were analyzed.

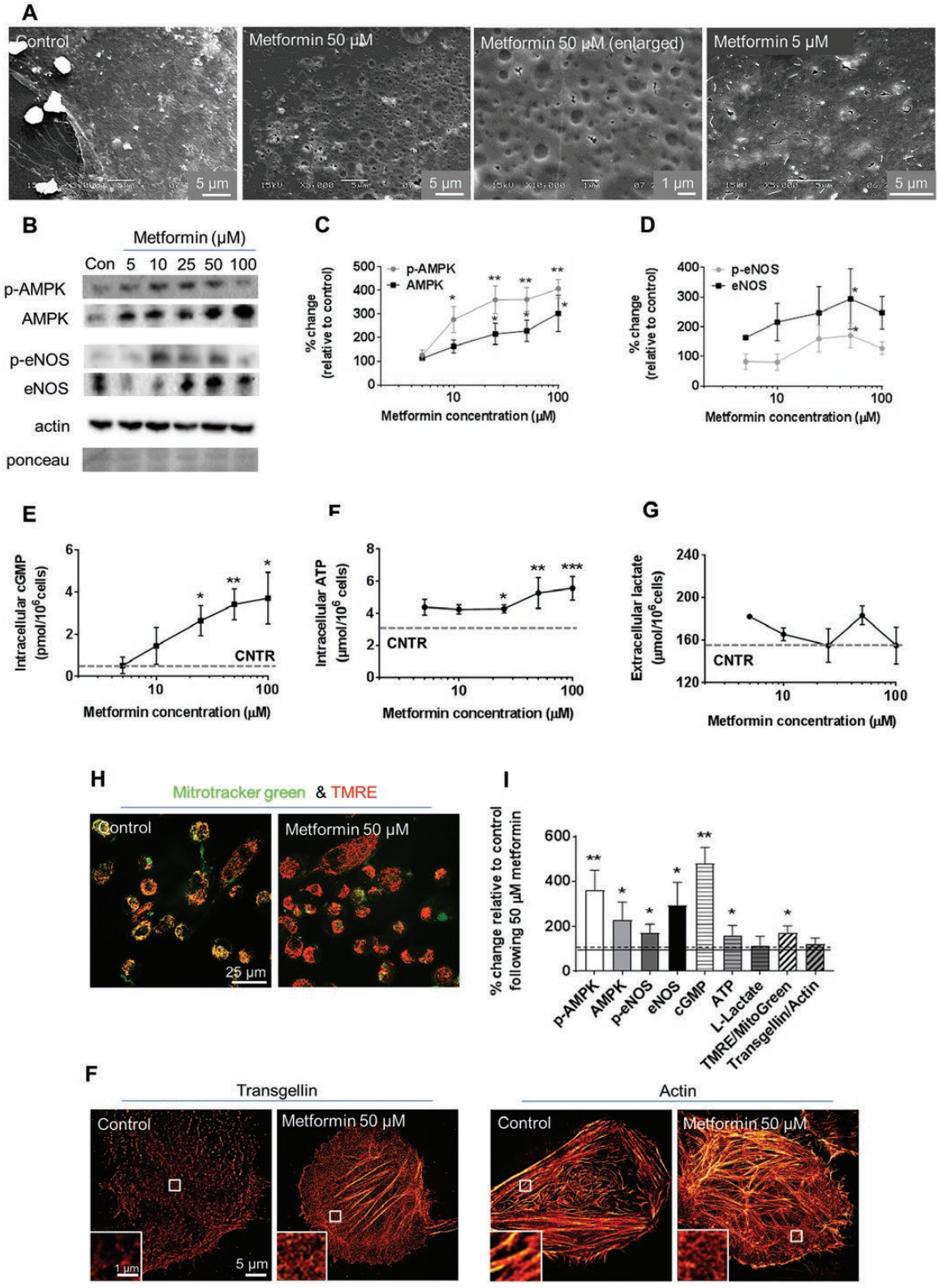

Figure 3. Effects of metformin treatment on SK-Hep1 cell lines. (**a**) Representative scanning electron microscopy images of SK-Hep1 cells following metformin treatment. Scale bar shows 1 or 5 µm. (**b**) Changes in p-AMPK, AMPK, p-eNOS, NOS, actin, and Ponceau protein expression as determined by western blot following metformin treatment. 10^7 cells were analyzed per sample. (**c–d**) Dose–response curves showing the % fold change for p-AMPK and AMPK (**c**), p-eNOS and NOS (**d**) (normalized to actin) with increasing metformin treatment. Data shows the mean ± SD based on three to four (technical replicates) individual experiments. * indicates a *p*-value of < .05, ** $p < .01$ compared to control data. Statistics were performed using Kruskal–Wallis with post hoc Dunn's test to compare between groups. (**e–g**) Intracellular cGMP (**e**), ATP (**f**), and extracellular L-lactate (**g**) was determined by commercial assays. Dose–response curves are shown with changes in determinant relative to increasing metformin. Data shows the mean ± *SD*. Dotted line shows control (untreated) score. Intracellular

In Vivo Long-Term Studies in Mice

Three-month-old male C57/Bl6 mice (n = 4 per treatment group) were obtained from the Animal Resource Centre in Perth, Western Australia and housed at the Charles Perkins Centre (The University of Sydney, NSW, Australia). Mice were group housed, maintained on a 12-hour light/dark cycle, 20–25°C, 50%–60% relative humidity and provided with bedding, ventilated caging systems, and enrichment as per the ARRIVE guidelines. The metformin diet consisted of 1 mg metformin per 1 g of standard chow (0.1%). Standard chow had the macronutrient ratio of 19:18:63 (protein: fat: carbohydrate). Food and water were given ad libitum with food usage and mouse weights monitored every third day. Mice either euthanized at 3 months under anesthesia (xylazine 100 mg/kg ketamine, 10 mg/kg) or maintained on either the metformin- or control chow-diets for 12 months prior to being euthanized under anesthesia (xylazine 100 mg/kg ketamine, 10 mg/kg).

Insulin was measured using an ultra-sensitive mouse insulin ELISA kit according to the manufacturer's instructions. Ten microliters of blood were collected following fasting for 5 hours and following an oral bolus of 25% glucose solution from a tail vein snip/collection. Euthanasia of mice was performed following blood collection. SEM was performed on livers that had been fixed via portal vein perfusion as previous described (17–19).

Statistics

Statistical analyses between drug treatments experiments were performed comparing multiple groups using Kruskal–Wallis tests with a post hoc Dunn's method. A p-value of < .05 was deemed to be significant.

Results

Effects of Metformin on Isolated LSECs

LSECs from old mice had reduced fenestration porosity (young: 5.11 ± 0.11%; old: 3.05 ± 0.10%; p = .001) and frequency (young: 2.94 ± 0.10; old: 1.58 ± 0.11; p = .001) with no change in diameter (young: 143.54 ± 1.44 nm; old: 151.06 ± 5.70 nm; p = .27) compared to young mice (Figure 1a and d).

The effects of metformin on fenestrations in LSECs isolated from young and old mice are shown in Figure 1. In LSECs from both young and old mice, there was a dose-dependent increase in fenestration porosity which was maximal at 50 µM metformin (Figure 1a and d) where porosity was increased by 25% in young mice (control: 5.11 ± 0.11%; metformin: 6.44 ± 0.34%; p = .05) and by 50% in old mice (control: 3.05 ± 0.11%; metformin: 4.70 ± 0.28%; p = .04). This dosage of metformin also increased fenestration frequency (Figure 1a and d) in the same manner (20% in young mice [control: 2.94 ± 0.10%; metformin: 3.53 ± 0.17%; p = .05]; 50% in old mice [control: 1.57 ± 0.10; metformin: 2.19 ± 0.15; p = .03]). Metformin did not alter fenestration diameter (Figure 1c).

The effect of metformin on fenestrations was reduced by pretreatment of LSECs with L-NAME, Compound C and Peptide 18 (Figure 1e and f). Cell viability was not influenced by age, metformin, or any of the inhibitors (L-NAME, Compound C, Peptide 18; Figure 1g). High dosages of metformin were associated with increased expression of transgelin in young mice only (p = .05; Figure 1h and i). Changes in the actin cytoskeleton were observed in LSECs from both young and old mice as evaluated by dSTORM (Figure 1h).

In Vivo Effects of Metformin

In vivo fenestration data demonstrated a similar age-related effect to isolated LSECs with reduced fenestration porosity (young 5.53 ± 1.2%; old 3.47 ± 0.45%; p = .02) and frequency (young: 6.78 ± 0.90; old: 4.67 ± 1.00; p = .02) with no change in diameter compared to young mice (Figure 2a and d). Mice fed 0.1% metformin for 12 months had a 30% increase in fenestration porosity (p = .02) and frequency (p = .05) compared to controls (Figure 2b and d). The use of 0.1% metformin diet reduced the age-related loss of fenestration porosity and frequency by 50%. These metformin-fed mice also demonstrated improvements in age-related changes in fasting and fed insulin levels (p < .05; Figure 2e). There were no differences in fasting or fed glucose levels; however, no age-related changes were observed (Figure 2f). There were no significant differences in body weight or lean mass (Figure 2g).

Effects of Metformin on SK-Hep1 Cells

SK-Hep1 cells developed fenestration-like structures following treatment with 50 µM metformin (Figure 3a). Treatment with 50 µM metformin was associated with increases in p-AMPK (n = 4; p = .01), AMPK (n = 4; p = .03), p-eNOS (n = 4; p = .05), NOS (n = 4; p = .04), cGMP (n = 3; p = .01), and ATP (n = 3; p = .05), which tended to be either dose-dependent or seen only at higher concentrations depending upon the substrate (Figure 3b–f and i). Metformin did not influence L-lactate levels (n = 3; p = .67) (Figure 3g and i). Mitotracker green and TMRE studies showed that metformin increased mitochondrial permeability potential (n = 3; p = .05; Figure 3h and i) while dSTORM revealed reorganization of actin but no changes in transgelin (n = 8; p = .78; Figure 3i and f).

Discussion

Metformin increased fenestrations in LSECs. The effect of metformin was seen in LSECs isolated from young and old mice that were treated in vitro with metformin. This effect was also seen in the livers from older mice that had been fed 0.1% metformin for 12 months. In both cases, there was a 30% or greater increase in fenestration porosity and frequency. These results are consistent with a previous study where mice were fed 1% metformin every-other-week for 17 weeks then euthanized at 24 months of age (20). In this study, we found that fenestration porosity and frequency in vivo was increased by about 30% with metformin. Aging is associated with a reduction in fenestrations

measurements were performed using 10^6 cells with 10^7 cells used for extracellular measurements were each experiment. Experiments were performed in triplicate. * indicates a p-value of < .05, ** p < .01, *** p < .001 compared to control data. Statistics were performed using Kruskal–Wallis with post hoc Dunn's test to compare between groups. (**h**) Sample images of immunofluorescent staining for Mitotracker green and TMRE (red) were performed following metformin drug treatments in RMPI media without phenol red. Scale bar shows 25 µm. (i) Summary of changes induced by 50 µM metformin treatment on SK-Hep1 cells. Data represented as a bar graph with the mean ± *SD*. The % change in expression of p-AMPK, AMPK, p-eNOS, eNOS, cGMP, ATP, L-lactate, TMRE/Mitotracker green, and Transgelin/Actin are shown relative to control. Densitometry was performed on images acquired from confocal and dSTORM; eight images were captured with data analysis was performed using Image J software. Images were converted to binary data with measurements taken across the whole cell all other data was analysis as described in **c–g**. (**f**) dSTORM images show transgelin and actin cytoskeleton morphology changes promoted by metformin drug treatment in young mice. Images were produced following 40,000 image collections and processed using RapidSTORM software. Scale bar shown 5 µm.

in LSECs, along with several other changes in the endothelium that have been termed "pseudocapillarization." Metformin appears to be able to prevent age-related defenestration with chronic treatment, and reverse age-related defenestration with acute treatment.

Metformin is thought to influence aging via its effects on nutrient sensing pathways, particularly by activating AMPK. In this sense, it has been considered to be a calorie restriction-mimetic, that can replicate some of the beneficial effects of caloric restriction in ad libitum-fed animals. Therefore, it is of note that we have also found that caloric restriction prevents age-related defenestration and the other changes of pseudocapillarization (27). Metformin influences a broad range of age-related changes in animals (3,20,28) and there are now clinical trials planned to evaluate the effects of metformin on aging in humans (29). Our results indicate that the antiaging effects of metformin extend to the liver microvasculature. This has potential systemic implications. Fenestrations in LSECs provide a portal for the transfer of insulin and other substrates from the sinusoidal blood to the hepatocytes. In a previous study, we found that age-related loss of fenestrations directly contributed to hepatic insulin resistance and impaired insulin clearance in old mice and rats (14). By maintaining the patency of fenestrations, metformin would be expected to increase insulin clearance and the action of insulin on the liver. This is consistent with our finding that insulin levels were lower in mice on metformin and, of course, the well-established antidiabetic effects of metformin.

We also explored possible mechanistic pathways for the effects of metformin on fenestrations. In LSECs isolated from young mice, metformin increased fenestration porosity and frequency via a pathway that was dependent on pAMPK, eNOS/cGMP, and pMLCK/actin remodeling. We have highlighted in this study that all three of these pathways are required in regulating fenestrations following metformin treatment. These pathways are similar to those we and others have previously reported for several other agents that increase fenestrations in LSECs (19,30). We have previously reported that actin disruption influences fenestrations (19). Here we identified that transgelin, a protein that inhibits the polymerization of actin (31), is upregulated in young but not old mice following metformin treatment. This represents a novel pathway for the regulation of fenestrations and for the action of metformin. Lastly, metformin has been associated with lactic acidosis (32,33); therefore, we also investigated whether concentrations of 5–100 μM metformin had any impact on lactate production by the LSEC. There was no effect.

In this study, we examined the influence of metformin on SK-Hep1 cells which are an immortal human liver cell line with many characteristics of LSECs (34). Metformin was associated with the generation of fenestration-like structures and there was a concentration-dependent increase in p-AMPK, AMPK, and the ratio of p-AMPK/AMPK, consistent with the established effects of metformin on AMPK activation (6). We also demonstrated that metformin increased the expression of p-eNOS, NOS, and cGMP in SK-Hep1 cells. Metformin is usually considered to be an inhibitor of mitochondrial function leading to AMPK activation via reduced levels of ATP. However, we found that metformin was associated with a small increase in intracellular ATP levels. It should be noted that inhibition of mitochondrial function by metformin is concentration-dependent and only has inhibitory effects at concentrations above 1–5 mM (3,35), which is 10-fold greater than the highest concentrations we utilized. Moreover, low-dose metformin increased mitochondrial complex I activity in the livers of mice (3). Within LSECs, fenestrations are dependent upon actin remodeling, which requires ATP (36); therefore, any increase in ATP with metformin might promote fenestration formation. Furthermore, this result suggests that the effects of metformin on AMPK activation might not be entirely dependent upon decreased ATP levels, at least in SK-Hep1 cells. Further study is required to determine the changes in AMP relative to the increased ATP observed in this study.

We also demonstrated that metformin increased the expression of p-eNOS, NOS, and cGMP in SK-Hep1 cells. The production of nitric oxide is one of the other critical roles of LSECs that is reduced with age (see review by Maslak, Gregorius, Chlopicki (37)). Within the liver, nitric oxide is involved in the quiescence of hepatic stellate cells and regulation of hepatocytes (37). The restoration of a healthy LSEC phenotype (fenestrated and nitric oxide releasing) has been shown to prevent fibrosis progression and regression of fibrosis (38,39). This suggests that metformin via its actions on LSECs may be added to the beneficial effects of AMPK agonists for treating hepatic fibrosis (40).

It is important to note that there was a nonlinear concentration-dependent effect of metformin on fenestrations in isolated LSECs: The effect was maximal at 50 μM and then decreased at 100 μM. The concentrations of metformin that have the greatest beneficial effects on hepatocytes is in the range of 0.1–10 mM (8), well above those we found to be beneficial for fenestrations in LSECs. The direct effects of metformin on molecular pathways within LSECs have not been previously reported. Dose-dependent aging effects have been seen in mice, with 0.1% dietary metformin causing increased life expectancy while 1% dietary metformin reduced lifespan (3). In our study, long-term administration of 0.1% metformin in the diet was associated with increased fenestrations and lower insulin levels, consistent with the study showing that this dosage increases life span.

In conclusion, metformin was found to increase fenestration porosity and frequency in LSECs isolated from both young and old mice, via a pathway dependent on AMPK, NOS/cGMP, and MLCK/actin remodeling in vitro. Long-term treatment with metformin increased fenestrations in old mice which was associated with lower insulin levels. Along with its many other actions, metformin ameliorates age-related changes in the LSEC which might contribute to its effects on age-related insulin sensitivity.

Funding

The study was supported by the Australian National Health and Medical Research Council Projects #1141234 and #1101913; the Ageing and Alzheimer's Research Foundation (a Division of the Medical Foundation of the University of Sydney); Sydney Medical School Foundation McKnight Bequest; the University of Sydney DVCR Research Equity Fellowship; and the University of Tromsø Faculty of Health Sciences travel grants to P.M. and H.M.

Conflict of Interest

None reported.

Author Contributions

Concept of study: N.H., P.M., D.L.C., V.C.; experimentation and analysis: N.H., G.L., S.K., T.P., X.C., H.M., P.M., G.C., J.W., F.L.C.; manuscript preparation: N.H., G.L., S.K., T.P., D.L.C., V.C.

References

1. Hunt NJ, McCourt PAG, Le Couteur DG, Cogger VC. Novel targets for delaying aging: the importance of the liver and advances in drug delivery. *Adv Drug Deliv Rev*. 2018;135:39–49. doi:10.1016/j.addr.2018.09.006

2. Barzilai N, Crandall JP, Kritchevsky SB, Espeland MA. Metformin as a tool to target aging. *Cell Metab*. 2016;23:1060–1065. doi:10.1016/j.cmet.2016.05.011
3. Martin-Montalvo A, Mercken EM, Mitchell SJ, et al. Metformin improves healthspan and lifespan in mice. *Nat Commun*. 2013;4:2192. doi:10.1038/ncomms3192
4. Rena G, Hardie DG, Pearson ER. The mechanisms of action of metformin. *Diabetologia*. 2017;60:1577–1585. doi:10.1007/s00125-017-4342-z
5. Shaw RJ, Lamia KA, Vasquez D, et al. The kinase LKB1 mediates glucose homeostasis in liver and therapeutic effects of metformin. *Science*. 2005;310:1642–1646. doi:10.1126/science.1120781
6. Zhou G, Myers R, Li Y, et al. Role of AMP-activated protein kinase in mechanism of metformin action. *J Clin Invest*. 2001;108:1167–1174. doi:10.1172/JCI13505
7. Howell JJ, Hellberg K, Turner M, et al. Metformin inhibits hepatic mTORC1 signaling via dose-dependent mechanisms involving AMPK and the TSC complex. *Cell Metab*. 2017;25:463–471. doi:10.1016/j.cmet.2016.12.009
8. Ford RJ, Fullerton MD, Pinkosky SL, et al. Metformin and salicylate synergistically activate liver AMPK, inhibit lipogenesis and improve insulin sensitivity. *Biochem J*. 2015;468:125–132. doi:10.1042/BJ20150125
9. Fullerton MD, Galic S, Marcinko K, et al. Single phosphorylation sites in Acc1 and Acc2 regulate lipid homeostasis and the insulin-sensitizing effects of metformin. *Nat Med*. 2013;19:1649–1654. doi:10.1038/nm.3372
10. Madiraju AK, Qiu Y, Perry RJ, et al. Metformin inhibits gluconeogenesis via a redox-dependent mechanism in vivo. *Nat Med*. 2018;24:1384–1394. doi:10.1038/s41591-018-0125-4
11. Towler MC, Hardie DG. AMP-activated protein kinase in metabolic control and insulin signaling. *Circ Res*. 2007;100:328–341. doi:10.1161/01.RES.0000256090.42690.05
12. Hilmer SN, Cogger VC, Fraser R, McLean AJ, Sullivan D, Le Couteur DG. Age-related changes in the hepatic sinusoidal endothelium impede lipoprotein transfer in the rat. *Hepatology*. 2005;42:1349–1354. doi:10.1002/hep.20937
13. Mitchell SJ, Huizer-Pajkos A, Cogger VC, et al. Age-related pseudocapillarization of the liver sinusoidal endothelium impairs the hepatic clearance of acetaminophen in rats. *J Gerontol A Biol Sci Med Sci*. 2011;66:400–408. doi:10.1093/gerona/glq221
14. Mohamad M, Mitchell SJ, Wu LE, et al. Ultrastructure of the liver microcirculation influences hepatic and systemic insulin activity and provides a mechanism for age-related insulin resistance. *Aging Cell*. 2016;15:706–715. doi:10.1111/acel.12481
15. Warren A, Bertolino P, Cogger VC, McLean AJ, Fraser R, Le Couteur DG. Hepatic pseudocapillarization in aged mice. *Exp Gerontol*. 2005;40:807–812. doi:10.1016/j.exger.2005.06.012
16. Le Couteur DG, Cogger VC, Markus AM, et al. Pseudocapillarization and associated energy limitation in the aged rat liver. *Hepatology*. 2001;33:537–543. doi:10.1053/jhep.2001.22754
17. Cogger VC, O'Reilly JN, Warren A, Le Couteur DG. A standardized method for the analysis of liver sinusoidal endothelial cells and their fenestrations by scanning electron microscopy [Video-audio media]. *J Vis Exp*. 2015;(98):e52698. doi:10.53791/52698
18. Svistounov D, Warren A, McNerney GP, et al. The relationship between fenestrations, sieve plates and rafts in liver sinusoidal endothelial cells. *PLoS One*. 2012;7:e46134. doi:10.1371/journal.pone.0046134
19. Hunt NJ, Lockwood GP, Warren A, et al. Manipulating fenestrations in young and old liver sinusoidal endothelial cells. *Am J Physiol Gastrointest Liver Physiol*. 2019;316:G144–G154. doi:10.1152/ajpgi.00179.2018
20. Alfaras I, Mitchell SJ, Mora H, et al. Health benefits of late-onset metformin treatment every other week in mice. *NPJ Aging Mech Dis*. 2017;3:16. doi:10.1038/s41514-017-0018-7
21. Detaille D, Guigas B, Chauvin C, et al. Metformin prevents high-glucose-induced endothelial cell death through a mitochondrial permeability transition-dependent process. *Diabetes*. 2005;54:2179–2187. doi:10.2337/diabetes.54.7.2179
22. Wolter S, Löschberger A, Holm T, et al. rapidSTORM: accurate, fast open-source software for localization microscopy. *Nat Methods*. 2012;9:1040–1041. doi:10.1038/nmeth.2224
23. Zolotarevsky Y, Hecht G, Koutsouris A, et al. A membrane-permeant peptide that inhibits MLC kinase restores barrier function in in vitro models of intestinal disease. *Gastroenterology*. 2002;123:163–172. doi:10.1053/gast.2002.34235
24. Víteček J, Lojek A, Valacchi G, Kubala L. Arginine-based inhibitors of nitric oxide synthase: therapeutic potential and challenges. *Mediators Inflamm*. 2012;2012:318087. doi:10.1155/2012/318087
25. Kang SW, Haydar G, Taniane C, et al. AMPK activation prevents and reverses drug-induced mitochondrial and hepatocyte injury by promoting mitochondrial fusion and function. *PLoS One*. 2016;11:e0165638. doi:10.1371/journal.pone.0165638
26. Fu D, Mitra K, Sengupta P, Jarnik M, Lippincott-Schwartz J, Arias IM. Coordinated elevation of mitochondrial oxidative phosphorylation and autophagy help drive hepatocyte polarization. *Proc Natl Acad Sci USA*. 2013;110:7288–7293. doi:10.1073/pnas.1304285110
27. Jamieson HA, Hilmer SN, Cogger VC, et al. Caloric restriction reduces age-related pseudocapillarization of the hepatic sinusoid. *Exp Gerontol*. 2007;42:374–378. doi:10.1016/j.exger.2006.11.004
28. Novelle MG, Ali A, Diéguez C, Bernier M, de Cabo R. Metformin: a hopeful promise in aging research. *Cold Spring Harb Perspect Med*. 2016;6:a025932. doi:10.1101/cshperspect.a025932
29. Barzilai N. Targeting aging with metformin (TAME). *Innov Aging*. 2017;1:743. doi:10.1093/geroni/igx004.2682
30. DeLeve LD. Liver sinusoidal endothelial cells in hepatic fibrosis. *Hepatology*. 2015;61:1740–1746. doi:10.1002/hep.27376
31. Han M, Dong LH, Zheng B, Shi JH, Wen JK, Cheng Y. Smooth muscle 22 alpha maintains the differentiated phenotype of vascular smooth muscle cells by inducing filamentous actin bundling. *Life Sci*. 2009;84:394–401. doi:10.1016/j.lfs.2008.11.017
32. Lazarus B, Wu A, Shin J-I, et al. Association of metformin use with risk of lactic acidosis across the range of kidney function: a community-based cohort study. *JAMA Intern Med*. 2018;178:903–910. doi:10.1001/jamainternmed.2018.0292
33. Rhee CM, Kovesdy CP, Kalantar-Zadeh K. Risks of metformin in type 2 diabetes and chronic kidney disease: lessons learned from Taiwanese data. *Nephron*. 2017;135:147–153. doi:10.1159/000450862
34. Cogger VC, Arias IM, Warren A, et al. The response of fenestrations, actin, and caveolin-1 to vascular endothelial growth factor in SK Hep1 cells. *Am J Physiol Gastrointest Liver Physiol*. 2008;295:G137–G145. doi:10.1152/ajpgi.00069.2008
35. Kane DA, Anderson EJ, Price JW III, et al. Metformin selectively attenuates mitochondrial H2O2 emission without affecting respiratory capacity in skeletal muscle of obese rats. *Free Radic Biol Med*. 2010;49:1082–1087. doi:10.1016/j.freeradbiomed.2010.06.022
36. Braet F, Muller M, Vekemans K, Wisse E, Le Couteur DG. Antimycin A-induced defenestration in rat hepatic sinusoidal endothelial cells. *Hepatology*. 2003;38:394–402. doi:10.1053/jhep.2003.50347
37. Maslak E, Gregorius A, Chlopicki S. Liver sinusoidal endothelial cells (LSECs) function and NAFLD; NO-based therapy targeted to the liver. *Pharmacol Rep*. 2015;67:689–694. doi:10.1016/j.pharep.2015.04.010
38. Deleve LD, Wang X, Guo Y. Sinusoidal endothelial cells prevent rat stellate cell activation and promote reversion to quiescence. *Hepatology*. 2008;48:920–930. doi:10.1002/hep.22351
39. Xie G, Wang X, Wang L, et al. Role of differentiation of liver sinusoidal endothelial cells in progression and regression of hepatic fibrosis in rats. *Gastroenterology*. 2012;142:918–927.e6. doi:10.1053/j.gastro.2011.12.017
40. Liang Z, Li T, Jiang S, et al. AMPK: a novel target for treating hepatic fibrosis. *Oncotarget*. 2017;8(37):62780–62792. doi:10.18632/oncotarget.19376